Hindawi
Journal of Control Science and Engineering
Volume 2017, Article ID 5401616, 15 pages
https://doi.org/10.1155/2017/5401616

Research Article

Two-Layer Linear MPC Approach Aimed at Walking Beam Billets Reheating Furnace Optimization

Silvia Maria Zanoli and Crescenzo Pepe

Dipartimento di Ingegneria dell'Informazione, Università Politecnica delle Marche, Ancona, Italy

Correspondence should be addressed to Silvia Maria Zanoli; s.zanoli@univpm.it

Received 23 September 2016; Revised 18 November 2016; Accepted 21 December 2016; Published 31 January 2017

Academic Editor: Shuyou Yu

In this paper, the problem of the control and optimization of a walking beam billets reheating furnace located in an Italian steel plant is analyzed. An ad hoc Advanced Process Control framework has been developed, based on a two-layer linear Model Predictive Control architecture. This control block optimizes the steady and transient states of the considered process. Two main problems have been addressed. First, in order to manage all process conditions, a tailored module defines the process variables set to be included in the control problem. In particular, a unified approach for the selection on the control inputs to be used for control objectives related to the process outputs is guaranteed. The impact of the proposed method on the controller formulation is also detailed. Second, an innovative mathematical approach for stoichiometric ratios constraints handling has been proposed, together with their introduction in the controller optimization problems. The designed control system has been installed on a real plant, replacing operators' mental model in the conduction of local PID controllers. After two years from the first startup, a strong energy efficiency improvement has been observed.

1. Introduction

In recent decades, process industries observed important changes and increasing need for technological improvements in the production units has been supported by an increasing level of automation. In this context, the migration toward more profitable control and optimization solutions has been registered, aimed at the research of optimal trade-offs between throughput and yields increasing, costs reduction, and product quality improvement [1].

In particular, a profitable balance between the meeting of precise production and quality specifications and the achievement of energy efficiency, complying with rigorous environmental standards, has to be ensured. For this purpose, minimum payback time solutions are preferred by process engineers and managers. These smart solutions aim at a maximum exploitation of the already existent devices: software strategies are preferred to hardware modifications, introducing Advanced Process Control (APC) systems [2, 3].

Among APC solutions, Model Predictive Control (MPC) architectures have shown their soundness and strong reliability in control and optimization of multivariable constrained industrial processes [4, 5]. MPC implementation in process industries is mainly due to its formulation flexibility: different cost functions, subject to different types of constraints, can be suitably designed [6, 7].

In this paper, a developed APC framework for the control and the optimization of a walking beam billets reheating furnace located in an Italian steel plant is described. In the control literature, different control solutions for this control problem have been proposed. In [8], a computer control system for optimization of reheating furnaces has been developed which contains functions for fuel optimization, based on carpet diagrams and delay strategy multipliers. A hybrid optimization setpoint strategy for reheating furnaces temperatures is proposed in [9], based on steady state zone temperature optimization and dynamic optimization performed by PID controllers. In [10], a dynamic model of the reheating furnace is derived using material and energy balances and a multivariable predictive controller design procedure is proposed. In [11], the potential of nonlinear MPC techniques to improve the temperature control of the metal slabs in a hot mill reheat furnace is explored; in

particular, a focus on energy consumption decreasing is presented. A Lyapunov-based MIMO state feedback controller is developed for slab temperatures in a continuous, fuel-fired reheating furnace in [12]. The controller modifies reference trajectories of furnace temperatures and is part of a cascade control scheme. In [13], a nonlinear MPC is designed for a continuous reheating furnace for steel slabs. Based on a first-principles mathematical model, the controller defines local furnace temperatures so that the slabs reach their desired final temperatures. In [14], an MPC based control method is developed for the accurate control of cooling temperature in a hot-rolled strip laminar cooling process exploiting a tailored extended Kalman filter to observe the spatial distribution of strip temperature in water cooling section.

The proposed approach is based on a two-layer linear MPC architecture and addressed tailored control specifications. In particular, the linear approach allowed limiting the computational burden while the introduction of two main control modes ensured an effective control system [15].

In this paper, two control requirements have been specifically addressed. First, a unified approach for the selection of the control inputs to exploit for control objectives fulfilment has been formulated for all process conditions. For this purpose, a suitable module has been introduced which tightly cooperates with a two-layer linear *MPC* block. Furthermore, a decoupling strategy developed by the authors in a previous work [16] has been suitably extended so to include a proper handling of all process conditions. Second, an innovative mathematical approach aimed at stoichiometric ratios constraints tightening has been proposed.

Accurate simulations have proven the validity of the proposed approaches. The successive implementation of the designed controller on the industrial process successfully replaced the operators' manual driving of local PID controllers.

The paper is organized as follows: the analyzed walking beam billets reheating furnace is accurately described in Section 2, together with the control specifications and the developed process modelling. Section 3 details the developed APC framework, explaining the functions of the various blocks and how the proposed solutions impact the formulations of the two MPC layers. Tuning procedures and simulation examples have been depicted in Section 4, while Section 5 describes observed field results. Finally, conclusions have been reported in Section 6.

2. The Studied Billets Reheating Furnace

This section discusses the analyzed industrial process, that is, a walking beam billets reheating furnace. This process represents the most significant phase of an Italian steel plant. Process features, together with the control requirements and the process modelling, are detailed.

2.1. Process Characterization. The production chain of the studied Italian steel industry is schematically depicted in Figure 1.

Raw materials, for example, waste steel products, are processed in the first phase, so as to obtain small steel bars at an intermediate stage of manufacture. These bars are called *billets*. In the investigated process, billets are characterized by a rectangular (0.20 [m] × 0.16 [m]) or a quadratic (0.16 [m] × 0.16 [m] or 0.15 [m] × 0.15 [m]) section and their length can be 4.5 [m] or 9 [m].

The billets are then introduced in a reheating furnace. The considered reheating furnace measures 24 [m] and it can contain up to 80 billets simultaneously. When they enter the furnace, the billets can be characterized by very different temperatures. These input temperatures vary from 30[°C] to 700[°C]. The billets that are inside the furnace are reheated based on specific temperature profiles. In this way, at the furnace exit, billets temperature can vary, according to the specifications of the subsequent rolling phase. Typical billet exit temperatures vary in the range of 1000[°C]–1100[°C]. After their path along the furnace, the billets are moved toward the rolling mill stands: here they are subjected to a plastic deformation, suitably performed by stands cylinders. These cylinders deform the reheated billets according to the finished products specifications. Examples of finished products are angle bars, iron rods, or tube rounds.

The present paper is focused on the reheating phase, that is, the crucial phase in a steel industry. The importance of this phase is due to the high energy amount required: in order to achieve energy efficiency, an optimal trade-off between conflicting requirements, that is, environmental impact decreasing, energy saving, and product and product quality increasing has to be ensured.

The reheating phase in a furnace is schematically represented in Figure 2: the billets are introduced in the considered reheating furnace from the left side and moved toward the outlet of the furnace by a revolving beam, according to the defined furnace production rate. This movement type names the considered reheating furnace as *walking beam* [17, 18]. Within the furnace, air/fuel burners (located on the furnace walls) trigger combustion reactions: in this way, thermal energy is transferred to the billets during their permanence in the furnace by radiation, convection, and conduction phenomena. In the considered plant, the fuel used is the natural gas. Inside reheating furnaces, it is typical to distinguish three different areas, that is, *Preheating*, *Heating*, and *Soaking area*, characterized by different billets phases of the reheating process. In turn, areas are divided into zones. Starting from the furnace entrance (Figures 2 and 3, left side), the furnace areas in the case at issue are as follows:

(i) *Preheating Area*. This furnace area is characterized by the absence of burners. This area, exploiting hot gasses from downstream areas, performs a billets preheating process. It is constituted by a single zone, called *tunnel* (Figure 3, "T"), with temperatures in the range 500[°C]–850[°C]. It is characterized by a length of 7 [m].

(ii) *Heating Area*. In this furnace area, the crucial phase of billets reheating process takes place. Here, the registered temperatures vary between 750[°C] and 1150[°C]. This area is divided into three zones, called (from the left side to the right side) *zone 5*, *zone 4*, and *zone 3*. Each zone is characterized by a length of 4 [m] and by the presence of 12 burners.

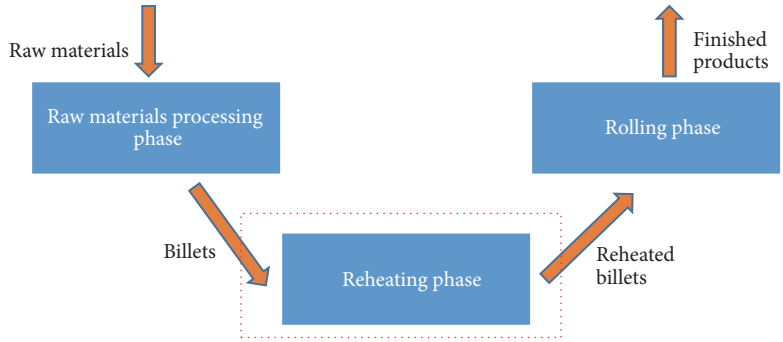

Figure 1: Workflow of the considered Italian steel industry.

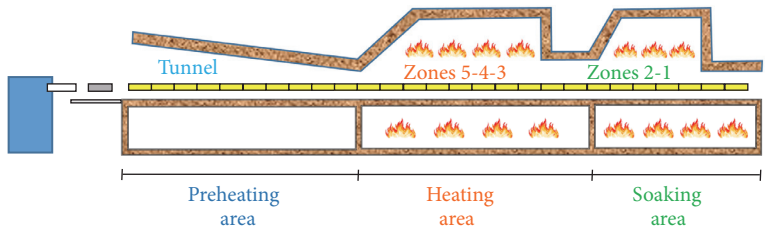

Figure 2: Representation of the considered walking beam billets reheating furnace.

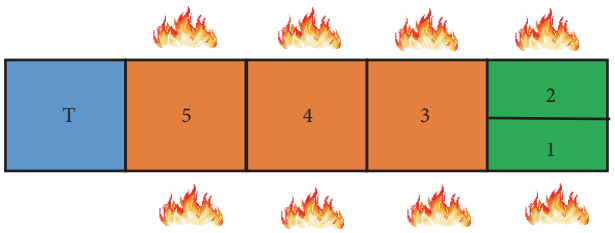

Figure 3: Schematic furnace zones disposition.

(iii) *Soaking Area*. In this last furnace area, the billets complete their reheating process. Here, temperatures vary approximately in the range 1100[°C]–1250[°C] and the total length is 5 [m]. The furnace area, equipped with 24 burners, is transversally divided into two zones, denoted as *zone 2* and *zone 1* (Figure 3).

Billets, during their traverse through the furnace, are subjected to monotonically increasing temperatures. At the beginning of the *Preheating area* is located a heat exchanger, denoted as *smoke-exchanger*. This allows the heat recover from the combustion smokes of the various furnace areas which is used for the preheating of the combustion air provided to each burner.

2.2. Process Instrumentation and Control Requirements. In the considered reheating furnace, measurements of the temperature of each furnace zone and of the smoke-exchanger are acquired by thermocouples suitably positioned within the furnace. The *Heating* and *Soaking* furnace *areas* are equipped with flowmeters for fuel (natural gas) and air flow rates measurement. Air and furnace pressure are measured by manometers. The billets temperature at their entrance in the furnace are registered by an optical pyrometer. An additional pyrometer measures the temperature of the processed billets. Billets transition at the furnace inlet and outlet is detected by photocells.

Before the introduction of the proposed APC system, the reheating furnace was regulated by plant operators' manual conduction of local PID controllers. Operators, based on the furnace conditions and on the production requirements, set the zones temperature targets manually.

A great amount of thermal energy is required in a steel billets reheating furnace. With the previous control system, the natural gas consumption, per year, was about 9 million [Sm^3], related to a total steel production of approximately 35000 [ton]. The minimization of the fuel consumption, together with the furnace production rate maximization, clearly represents the crucial factor for energy efficiency achieving and improvement. In addition to these requirements, there is also the need to meet stringent quality standards of the finished products.

After an initial study and analysis phase, repeated and targeted meetings with plant managers, engineers, and operators were conducted and the following main control specifications have been outlined for the considered APC design [19, 20]:

(I) Compliance with the required billets temperature constraints at their exit from the furnace, based on the specifications for the subsequent plastic deformation in the rolling mill phase.

(II) Meeting of stoichiometry constraints related to air/fuel ratios.

(III) Meeting of total air flow rate and smoke-exchanger temperature limits, so as to preserve furnace safety.

Table 1: The Manipulated Variables.

Variable name	Acronym [units]
Zone i fuel flow rate ($i = 1, \ldots, 5$)	Fuel_i [Nm^3/h]
Zone i air flow rate ($i = 1, \ldots, 5$)	Air_i [Nm^3/h]

Table 2: The Disturbance Variables.

Variable name	Acronym [units]
Furnace production rate	Prod [t/h]
Furnace pressure	FurnPress [mm/H_2O]
Air pressure	AirPress [mbar]

Table 3: The main Controlled Variables.

Variable name	Acronym [units]
Tunnel temperature	Tun [°C]
Zone i ($i = 1, \ldots, 5$) temperature	Temp_i [°C]
Zone 1–zone 2 temp. difference	Diff 12 [°C]
Total air flow rate	AirTot [Nm^3/h]
Smoke-exchanger temperature	SE [°C]

(IV) Furnace management in all predictable conditions.

(V) Minimization of the fuel (natural gas) consumption, optimizing all furnace conditions (e.g., with a varying furnace production rate).

The simultaneous meeting of all the above requirements is not easily attainable by a manual conduction of the furnace. In the conduction of the reheating furnace, operators typically neglected the aspects more strictly tied to energy saving and environmental impact decreasing, being concentrated on assuring a suitable billets heating profile. So, with the previous furnace management, billets were often reheated more than needed by the subsequent rolling mill phase.

2.3. Modelling the Considered Process. In order to design an APC system for furnace energy efficiency improvement, an accurate process modelling has been performed. As widely used in APC applications, three main groups of process variables have been identified: Controlled Variables (CVs), Manipulated Variables (MVs), and Disturbance Variables (DVs). CVs are the process outputs (assumed all measured): their control is performed exploiting MVs and taking into account DVs information, in a feedforward way. In fact, MVs and DVs represent the measured process inputs: the APC system can only act on MVs, while DVs cannot be modified by the APC system. CVs have been included in a $y_{[m_y \times 1]}$ vector; MVs and DVs have been grouped in a $u_{[l_u \times 1]}$ vector and in a $d_{[l_d \times 1]}$ vector, respectively. Tables 1 and 2 depict MVs and DVs, while key CVs have been reported in Table 3. In the CVs group, the following process variables have been included: the temperature of each furnace zone (including tunnel), the difference between zone 1 and zone 2 temperatures, the smoke-exchanger temperature, the total air flow rate, and the fuel and air valves opening (per cent). In the DVs group, furnace production rate, air pressure, and furnace pressure have been included. Finally, in the MVs group, air and fuel flow rates of each furnace zone have been considered. In the plant configuration, fuel and air flow rates are regulated through PID controllers: the designed APC system will provide the PID low level controllers with suitable set-points. Their computation will be described in Section 3.

An identification procedure based on a black-box approach has been conducted, in order to obtain accurate dynamical models that could describe the selected process inputs (MVs/DVs) and outputs (CVs) behaviour [21–23]. First-order strictly proper asymptotically stable linear time invariant models without delays have been obtained. In these models, deviations of the process variables from consistent operating points have been included. Tables 4 and 5 symbolically represent the CVs-MVs and CVs-DVs gain matrices, $G_{yu\,[m_y \times l_u]}$ and $G_{yd\,[m_y \times l_d]}$: the gain sign of the transfer functions that relate the MVs-DVs with the main CVs is here reported. Exploiting the identified models, billets temperature can be controlled with a suitable constrained control of the furnace zones temperature and of the temperature difference between the last two furnace zones (specification (I) in Section 2.2). Furthermore, smoke-exchanger temperature and total air flow rate can be controlled through fuel and air flow rates (specification (III) in Section 2.2). With regard to fuel and air flow rates usage, plant engineers have agreed on three additional requirements:

(i) The temperature of all the furnace zones, except tunnel, must be controlled exploiting only the related fuel flow rate.

(ii) The temperatures of the tunnel and of the smoke-exchanger must be controlled exploiting only zone 5 and zone 4 fuel flow rates.

(iii) The total air flow rate must be regulated using only zone 5 and zone 4 air flow rates.

In order to fulfil these additional objectives, an extended decoupling strategy has been developed by the authors (Sections 3.2 and 3.3).

Each of the furnace zones equipped with burners must comply with stoichiometric constraints, in order to guarantee proper thermodynamic reactions. In the considered case study, five stoichiometric ratios have to be controlled. These variables have been grouped in $z_{[m_z \times 1]}$ vector of *ratio* Controlled Variables (rCVs). Typical lower and upper constraints for the considered stoichiometric ratios have been summarized in Table 6. The stoichiometric ratios lower constraints represent safety conditions: their excessive violation can lead to a furnace stop. The upper constraints avoid air excess in the burners' combustion, contributing to the achievement of furnace energy efficiency. Stoichiometric ratios constraints have been suitably handled by an innovative formulation in the *MPC* block (Section 3.5).

The proposed extended decoupling strategy, together with additional procedures, allows the optimization of all furnace conditions, searching for fuel minimization directions.

Table 4: The CVs-MVs mapping matrix.

Acronym	$Fuel_5$	$Fuel_4$	$Fuel_3$	$Fuel_2$	$Fuel_1$	Air_5	Air_4	Air_3	Air_2	Air_1
Tun	+	+	+	+	+					
$Temp_5$	+	+	+	+	+	−				
$Temp_4$		+	+	+	+		−			
$Temp_3$			+	+	+			−		
$Temp_2$				+	+				−	
$Temp_1$				+	+					−
Diff 12				−	+					
AirTot						+	+	+	+	+
SE	+	+	+	+	+					

Table 5: The CVs-DVs mapping matrix.

Acronym	Prod	FurnPress	AirPress
Tun	−	+	−
$Temp_5$	−	+	−
$Temp_4$	−	+	−
$Temp_3$	−	+	−
$Temp_2$	−	+	−
$Temp_1$	−	+	−
Diff 12			
AirTot			
SE	−	+	−

Table 6: The ratio Controlled Variables constraints.

Variable name	Acronym [units]	Lower constraint	Upper constraint
Zone 5 stoichiometric ratio	R_5 []	10.8	12.3
Zone 4 stoichiometric ratio	R_4 []	10.5	12
Zone 3 stoichiometric ratio	R_3 []	10.5	12
Zone 2 stoichiometric ratio	R_2 []	9.8	11.3
Zone 1 stoichiometric ratio	R_1 []	9.8	11.3

3. APC Framework

This section describes the APC framework designed for the control and the optimization of the considered walking beam reheating furnace. The various blocks are differentiated, together with their functions. In particular, the proposed control solutions are detailed.

3.1. Detailing the Scheme. The APC architecture has been depicted in Figure 4. Three main blocks can be noted: *Plant & SCADA* (*P&S*) block, *Data Conditioning & Decoupling Selector* (*DC&DS*), and *MPC* block.

At each control instant k, *P&S* block, based on a Supervisory Control and Data Acquisition (SCADA) system, supplies updated MVs, DVs, and CVs measurements ($u(k-1)$, $d(k-1)$, $y(k)$). Additionally, a status value (u-d-y-z status) for each process variable is forwarded.

DC&DS block detects abnormal situations, exploiting field data conditioning information, and defines the final status value for each variable (u-d-y status, z status), suitably processing *P&S* status information. Depending on the variable final status, the variables set to be included in the controller formulation at the current control instant is accordingly modified. Details about status handling have been explained by the authors in [24]. In this work, an extension of a decoupling strategy proposed by the authors in a previous work ([16]) is formulated, assuring a straight relationship between the decoupling strategy and the MVs and CVs status values definition (Decoupling Matrix). In this way, a unified approach for the selection of MVs to exploit for the fulfilment of CVs specifications has been guaranteed in all process conditions (Section 3.2).

The acquired information is forwarded to the linear Model Predictive Control (*MPC*) block characterized by a two-layer architecture. This block is constituted by the Targets Optimizing and Constraints Softening (TOCS) module at the upper level and the Dynamic Optimizer (DO) module at the lower lever, both supported by the Predictions Calculator module. These modules suitably cooperate, computing the MVs value $u(k)$ to be applied to the plant at the current control instant.

In both optimization problems, MVs constraints are assumed as *hard constraints*: they can never be violated and their feasibility has been suitably imposed. As widely used in MPC applications, CVs constraints are assumed as *soft constraints*: their *softening* is admitted in critical situations through the introduction of suitable nonnegative slack variables vectors, denoted by ε. An ad hoc approach has been dedicated to rCVs constraints, as it will be shown in Section 3.5.

3.2. Data Conditioning & Decoupling Selector Module Tasks. An APC system must properly handle process variables in all process conditions. The control system design has to take into account all detectable situations. Certain MVs, DVs, CVs, or rCVs must be excluded from the controller formulation, based on abnormal situations (e.g., bad conditions or local control loop faults) detection or on specific plant needs.

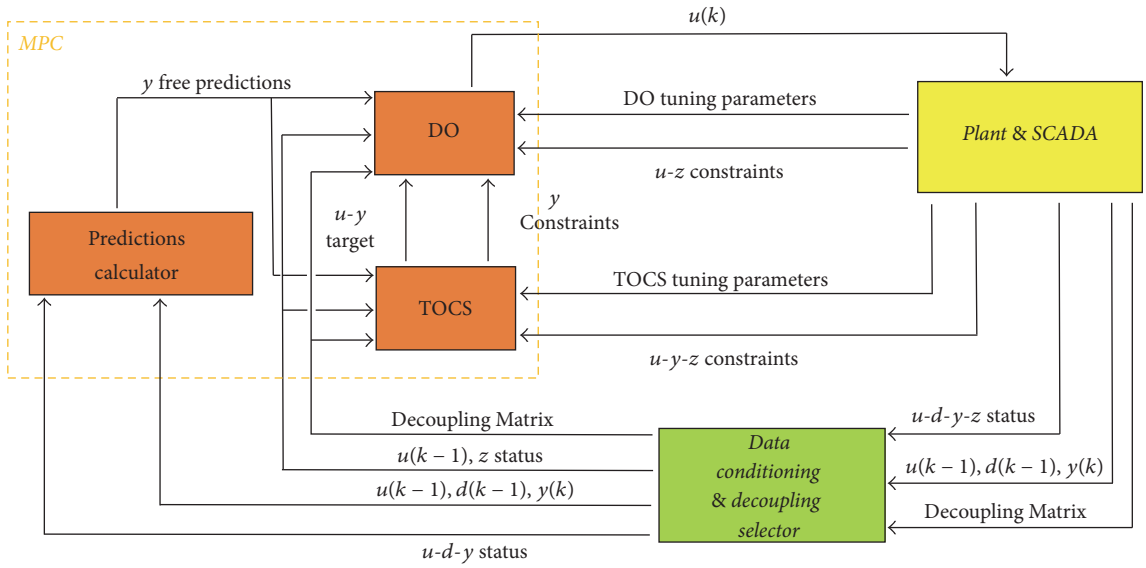

Figure 4: Architecture of the designed APC framework.

In the designed APC scheme, *DC&DS* block includes logics aimed at a proper modification of the initial status values supplied by *P&S* block (Figure 4, *u-d-y-z* status) as a consequence, for example, of spikes or freezing percentage violation [24]. These logics determine the final status values of all process variables (Figure 4, *z* status and *u-d-y* status).

In this work, two status values have been considered: *active* and *inactive*. An *active* MV is used by *MPC* block for control purposes while an *inactive* MV cannot be moved by *MPC* block: for future predictions of the system behaviour, its value is frozen to its last plant measurement (Figure 4, $u(k-1)$). When a CV (or a rCV) is *active*, *MPC* block acts for the satisfaction of the related control specifications, while, when a CV (or a rCV) is *inactive*, its control requirements must be ignored by *MPC* block.

As stated in Section 2, MVs/DVs-CVs relationships have been modelled with a linear time invariant asymptotically stable model without delays.

In order to include status value information on the process model, a $B_{yu\,[m_y \times l_u]}$ matrix has been introduced: a nonzero entry on the generic (i, j) element represents a nonzero relationship between the jth MV and the ith CV. Considering the gain matrix G_{yu} and defining with $\mathrm{op}_{\neq}(\cdot,\cdot)$ the element-wise inequality logical operation between two matrices, the binary matrix B_{yu} is obtained:

$$B_{yu} = \mathrm{op}_{\neq}\left(G_{yu}, 0_{[m_y \times l_u]}\right), \tag{1}$$

where $0_{[m_y \times l_u]}$ is a matrix with elements all equal to 0.

For the generic ith CV, if this CV is *active* at the current control instant, all *active* MVs tied to it (i.e., the *active* MVs characterized by a 1 on the related position on the ith row of B_{yu} matrix) can act for its specifications fulfilment. In order to admit additional degrees of freedom for the control specifications, in a previous work, the authors proposed a suitable decoupling strategy, not dependent on the tuning parameters. This strategy enables, for each CV, the selection of the MVs to exploit for its control purposes, that is, equivalently, the inhibition of given MVs.

Two equivalent mathematical approaches have been formulated [16]. In this work, the formulation based on the definition of a Decoupling Matrix is considered and suitably extended.

An initial Decoupling Matrix $D_{E[m_y \times l_u]}$ is supplied by *P&S* block (Figure 4). The generic (i, j) element of D_E is set equal to 0 if both the following conditions hold:

(i) The (i, j) element of B_{yu} matrix is equal to 1.

(ii) The jth MV must not be used to control the ith CV.

Otherwise, the (i, j) element is equal to 1.

The generic (i, j) nonzero element of the initial D_E matrix is zeroed by *DC&DS* block if at least one of the two following conditions holds:

(i) The ith CV is *inactive*.

(ii) The jth MV is *inactive*.

The final D_E matrix is then forwarded to TOCS and DO modules.

In the considered case study, rCVs are represented by the ratio between the related air and fuel flow rates. *DC&DS* block processes the rCVs status value supplied by *P&S* block, taking into account the final status values of air and fuel flow rates (Figure 4, *u-d-y* status). In this way, the final status value associated with each rCV is obtained (Figure 4, *z* status). Generally, the ith stoichiometric ratio ($i = 1, \ldots, 5$) is defined as *inactive* if the ith fuel flow rate is *inactive*. This means that if the ith fuel flow rate is *inactive*, the constraints of the ith stoichiometric ratio must be ignored by *MPC* block.

3.3. Predictions Calculator and TOCS Modules Tasks. As stated before, *MPC* block is composed of three modules.

The two-layer linear MPC scheme exploits process variables predictions on a *prediction horizon* H_p; these predictions are parametrized on a defined number of MVs moves (assumed here to be applied at the first H_u prediction steps), called *control horizon* and denoted with H_u $(0 < H_u \leq H_p)$ [25]. At each control instant, a sequence of MVs values is computed, but only the first value (Figure 4, $u(k)$) is forwarded to the plant, repeating the entire control algorithm at the next control instant (*receding horizon* strategy) [26, 27].

Predictions Calculator module computes CVs *free predictions* over H_p (Figure 4, y free predictions), keeping MVs and DVs constant at their last field value (Figure 4, $u(k-1)$ and $d(k-1)$, resp.) and taking into account the last CVs value (Figure 4, $y(k)$) for plant-model mismatch inclusion. Future information about DVs is assumed unknown, so future DVs trends are assumed constant at $d(k-1)$ value. In CVs *free predictions* computation, CVs status values information is also included.

For the generic vth CV, predictions over H_p are expressed by

$$\widehat{y}_v(k+i \mid k) = \widehat{y}_{\text{free}_v}(k+i \mid k) + \Delta\widehat{y}_v(k+i \mid k) \tag{2}$$

$$\Delta\widehat{y}_v(k+i \mid k) = F_{i,v} \cdot \Delta U(k) \tag{3}$$

$$\Delta U(k) = \begin{bmatrix} \Delta\widehat{u}(k \mid k) \\ \Delta\widehat{u}(k+1 \mid k) \\ \vdots \\ \Delta\widehat{u}(k+H_u-1 \mid k) \end{bmatrix}, \tag{4}$$

where $\widehat{y}_{\text{free}_v}(k+i \mid k)$ is the *free prediction* at the ith prediction instant, while $\Delta\widehat{y}_v(k+i \mid k)$ is the related *forced* component. $\Delta U(k)_{[l_u \cdot H_u \times 1]}$ is a vector that contains the H_u MVs moves $\Delta\widehat{u}(k+j \mid k)$ $(j = 0, \ldots, H_u - 1)$, assumed in the first H_u steps. $\Delta\widehat{u}(k+j \mid k)$ terms are among the decision variables of DO optimization problem (Section 3.4). The effects of MVs moves on the ith prediction are modelled by $F_{i,v\,[1 \times l_u \cdot H_u]}$ vector.

In this work, the prediction horizon H_p is assumed to be tuned so as to guarantee steady state reaching to the process model. Based on this assumption, the following relationship holds:

$$G_{yu} = \begin{bmatrix} F_{H_p,1}(1, (j-1) \cdot l_u + 1 : j \cdot l_u) \\ \vdots \\ F_{H_p,m_y}(1, (j-1) \cdot l_u + 1 : j \cdot l_u) \end{bmatrix} \quad (j = 1, \ldots, H_u), \tag{5}$$

where $F_{H_p,v}(1, (j-1) \cdot l_u + 1 : j \cdot l_u)$ $(v = 1, \ldots, m_y)$ is a subvector of $F_{H_p,v}$ of l_u columns, from the $((j-1) \cdot l_u + 1)$th to the $(j \cdot l_u)$th.

The two-layer linear MPC scheme performs two optimization problems: the first is solved by the upper layer, represented by TOCS module, while the second is related to the lower layer, that is, DO module. The formulation of the two modules is based on the same linear process model: TOCS module considers it in a steady state way, while both steady and transient states are taken into account by DO module.

In TOCS module formulation, MVs steady state value, denoted by $\widehat{u}_{\text{TOCS}}(k)$, is expressed by

$$\widehat{u}_{\text{TOCS}}(k) = u(k-1) + \Delta\widehat{u}_{\text{TOCS}}(k), \tag{6}$$

where $\Delta\widehat{u}_{\text{TOCS}}(k)$ represents the MVs steady state move: this vector is among decision variables of TOCS optimization problem. CVs steady state value, indicated by $\widehat{y}_{\text{TOCS}}(k)$, is expressed by

$$\widehat{y}_{\text{TOCS}}(k) = \begin{bmatrix} \widehat{y}_1(k+H_p \mid k) \\ \vdots \\ \widehat{y}_{m_y}(k+H_p \mid k) \end{bmatrix} = \widehat{y}_{\text{free}}(k+H_p \mid k) + \Delta\widehat{y}_{\text{TOCS}}(k) \tag{7}$$

$$\Delta\widehat{y}_{\text{TOCS}}(k) = G_{yu} \cdot \Delta\widehat{u}_{\text{TOCS}}(k), \tag{8}$$

where the CVs steady state forced component is represented by $\Delta\widehat{y}_{\text{TOCS}}(k)$.

When introducing the proposed extended decoupling strategy in the CVs steady state expression, (8) is modified as follows:

$$\Delta\widehat{y}_{\text{TOCS}}(k) = \left(G_{yu} \circ D_E\right) \cdot \Delta\widehat{u}_{\text{TOCS}}(k), \tag{9}$$

where $\circ$ indicates the element-wise product between matrices. In this way, information about MVs and CVs status values and additional control requirements are included. In this specific case, the additional control requirements are specifications (i)–(iii) of Section 2.3.

At each control instant, TOCS module minimizes a linear cost function, subject to linear constraints, based on (6), (7), and (9):

$$V_{\text{TOCS}}(k) = {c_u}^T \cdot \Delta\widehat{u}_{\text{TOCS}}(k) + {\rho_{y\_\text{TOCS}}}^T \cdot \varepsilon_{y\_\text{TOCS}} \tag{10}$$

subject to

$$\begin{aligned} &\text{(i)} \quad \text{lb}_{du\_\text{TOCS}} \leq \Delta\widehat{u}_{\text{TOCS}}(k) \leq \text{ub}_{du\_\text{TOCS}} \\ &\text{(ii)} \quad \text{lb}_{u\_\text{TOCS}} \leq \widehat{u}_{\text{TOCS}}(k) \leq \text{ub}_{u\_\text{TOCS}} \\ &\text{(iii)} \quad \text{lb}_{y\_\text{TOCS}} - \text{ECR}_{\text{lb}y\_\text{TOCS}} \cdot \varepsilon_{y\_\text{TOCS}} \leq \widehat{y}_{\text{TOCS}}(k) \\ &\qquad \leq \text{ub}_{y\_\text{TOCS}} + \text{ECR}_{\text{ub}y\_\text{TOCS}} \cdot \varepsilon_{y\_\text{TOCS}} \\ &\text{(iv)} \quad \text{TOCS } z \text{ constraints} \\ &\text{(v)} \quad \varepsilon_{y\_\text{TOCS}} \geq 0, \end{aligned} \tag{11}$$

where $\text{ub}_{du\_\text{TOCS}}$ and $\text{lb}_{du\_\text{TOCS}}$ represent the upper and lower constraints related to the MVs steady state move, while $\text{ub}_{u\_\text{TOCS}}$, $\text{lb}_{u\_\text{TOCS}}$ and $\text{ub}_{y\_\text{TOCS}}$, $\text{lb}_{y\_\text{TOCS}}$ are the upper and lower constraints for MVs and CVs steady state value, respectively. A set of ad hoc rCVs steady state linear constraints is represented by TOCS z constraints. Their inclusion in TOCS

module is detailed in Section 3.5. All these constraints are among u-y-z constraints of Figure 4. $c_{u[l_u \times 1]}$ vector weights MVs steady state move.

In TOCS optimization problem for each CV, two slack variables have been assumed (upper and lower constraints are not dependent). $\varepsilon_{y\_\mathrm{TOCS}\,[2 \cdot m_y \times 1]}$ is included in TOCS CVs constraints (11)(iii) suitably weighted by Equal Concern for the Relaxation (ECR) positive coefficients, while, in TOCS linear cost function (10), a positive column vector ρ_{y_TOCS} weights its effects.

TOCS tuning parameters of Figure 4 include c_u, ρ_{y_TOCS}, $\mathrm{ECR}_{\mathrm{lb}y\_\mathrm{TOCS}}$, and $\mathrm{ECR}_{\mathrm{ub}y\_\mathrm{TOCS}}$ terms.

Information about MVs and CVs status values and about the considered additional control specifications has been included in CVs steady state prediction through (9). In order to include this information in the other crucial terms of TOCS Linear Programming (LP) problem, the following column vectors are defined:

$$p_u = \mathrm{op}_{\neq}\left(\sum_{i=1}^{m_y} D_E(i,:)^T, 0_{[l_u \times 1]}\right),$$
$$p_y = \mathrm{op}_{\neq}\left(\sum_{j=1}^{l_u} D_E(:,j), 0_{[m_y \times 1]}\right), \tag{12}$$

where $D_E(i,:)$ and $D_E(:,j)$ represent the ith row and the jth column of D_E matrix, respectively. $0_{[n \times 1]}$ represents a vector of zeros. p_u is a $[l_u \times 1]$ vector, while p_y is a $[m_y \times 1]$ vector. The initial c_u vector is modified as follows:

$$c_u = c_u \circ p_u. \tag{13}$$

Furthermore, considering p_u, when its jth generic element ($j = 1, \ldots, l_u$) is equal to zero, all the upper and lower constraints related to the jth MV in (11)(i)-(11)(ii) are cut off by TOCS module. Similarly, taking into account p_y, when its ith generic element ($i = 1, \ldots, m_y$) is equal to zero, all the upper and lower constraints related to the ith CV in (11)(iii) are cut off by TOCS module.

TOCS module, solving its LP problem, computes the decision variables vector, constituted by $\Delta\widehat{u}_{\mathrm{TOCS}}(k)$ and $\varepsilon_{y\_\mathrm{TOCS}}$. Through expressions (6), (7), and (9), $\widehat{u}_{\mathrm{TOCS}}(k)$ and $\widehat{y}_{\mathrm{TOCS}}(k)$ are obtained: these vectors represent MVs and CVs steady state targets which are consistent with TOCS computed constraints. They are forwarded to DO module (Figure 4, u-y target). In order to guarantee a coherency between CVs steady state targets and constraints, the initial CVs constraints provided by *Pe&S* block to TOCS module (Figure 4, u-y-z constraints) are suitably processed taking into account $\varepsilon_{y\_\mathrm{TOCS}}$ values. The resulting CVs constraints over H_p are then forwarded to DO module (Figure 4, y constraints) [28].

3.4. DO Module Tasks. DO module represents the lower layer of the proposed MPC scheme. It solves the second optimization problem of *MPC* block, computing the MVs value that will be applied to the plant at each control instant.

In order to include the proposed extended decoupling strategy in the CVs predictions over H_p, (3) is modified as follows:

$$\Delta\widehat{y}_v(k+i \mid k) = \left(F_{i,v} \circ \left(1_{[1 \times H_u]} \otimes D_E(v,:)\right)\right) \cdot \Delta U(k), \tag{14}$$

where $1_{[1 \times H_u]}$ represents a vector of ones and $\otimes$ indicates the Kronecker product. In this way, the forced component of CVs dynamic expression (2) contains also information about MVs and CVs status values and additional control requirements.

At each control instant, DO module minimizes a quadratic cost function, subject to linear constraints, based on (2), (4), and (14):

$$V_{\mathrm{DO}}(k) = \sum_{i=1}^{H_p} \left\| \widehat{y}(k+i \mid k) - y_t(k+i \mid k) \right\|^2_{Q(i)} + \sum_{i=0}^{H_p-1} \left\| \widehat{u}(k+i \mid k) - u_t(k+i \mid k) \right\|^2_{S(i)} + \sum_{i=0}^{H_u-1} \left\| \Delta\widehat{u}(k+i \mid k) \right\|^2_{R(i)} + \left\| \varepsilon_{\mathrm{DO}}(k) \right\|^2_{\rho_{\mathrm{DO}}} \tag{15}$$

subject to

(i) $\mathrm{lb}_{du\_\mathrm{DO}}(i) \le \Delta\widehat{u}(k+i \mid k) \le \mathrm{ub}_{du\_\mathrm{DO}}(i), \quad i = 0, \ldots, H_u - 1$

(ii) $\mathrm{lb}_{u\_\mathrm{DO}}(i) \le \widehat{u}(k+i \mid k) \le \mathrm{ub}_{u\_\mathrm{DO}}(i), \quad i = 0, \ldots, H_u - 1$

(iii) $\mathrm{lb}_{y\_\mathrm{DO}}(i) - \mathrm{ECR}_{\mathrm{lb}y\_\mathrm{DO}}(i) \cdot \varepsilon_{\mathrm{DO}}(k) \le \widehat{y}(k+i \mid k) \le \mathrm{ub}_{y\_\mathrm{DO}}(i) + \mathrm{ECR}_{\mathrm{ub}y\_\mathrm{DO}}(i) \cdot \varepsilon_{\mathrm{DO}}(k), \quad i = 1, \ldots, H_p$ (16)

(iv) DO z constraints

(v) $\varepsilon_{\mathrm{DO}}(k) \ge 0,$

where $\mathrm{ub}_{du\_\mathrm{DO}}(i)$ and $\mathrm{lb}_{du\_\mathrm{DO}}(i)$ represent the upper and lower constraints related to MVs future dynamic moves $\Delta\widehat{u}(k+i \mid k)$ ($i = 0, \ldots, H_u - 1$), while $\mathrm{ub}_{u\_\mathrm{DO}}(i)$, $\mathrm{lb}_{u\_\mathrm{DO}}(i)$, and $\mathrm{ub}_{y\_\mathrm{DO}}(i)$, $\mathrm{lb}_{y\_\mathrm{DO}}(i)$ are the upper and lower constraints for MVs and CVs future dynamic values $\widehat{u}(k+i \mid k)$ ($i = 0, \ldots, H_u - 1$) and $\widehat{y}(k+i \mid k)$ ($i = 1, \ldots, H_p$), respectively. A set of ad hoc rCVs dynamic linear constraints is represented by DO z constraints. Their inclusion in DO module is detailed in Section 3.5. All these constraints are among u-z constraints and y constraints of Figure 4.

In this work, in DO optimization problem, a single slack variable for each CV or rCV is assumed. $\varepsilon_{\mathrm{DO}}(k)_{[(m_y+m_z) \times 1]}$ is included in DO CVs constraints (16)(iii) through suitable Equal Concern for the Relaxation (ECR) positive coefficients, while, in DO linear cost function (15), a positive definite diagonal matrix ρ_{DO} weights its effects.

$Q(i)$ and $S(i)$ in (15) are positive semidefinite diagonal matrices: they weight CVs and MVs future tracking errors,

respectively. Future tracking errors are evaluated with respect to the future reference trajectories represented by $y_t(k+i \mid k)$ and $u_t(k+i \mid k)$, respectively. $y_t(k+i \mid k)$ and $u_t(k+i \mid k)$ are suitably computed from CVs and MVs steady state targets, supplied by TOCS module. Finally, $R(i)$ are positive definite diagonal matrices that weight MVs moves over H_u. $Q(i)$, $S(i)$, $R(i)$, ρ_{DO}, $\mathrm{ECR}_{\mathrm{lb}y\_\mathrm{DO}}(i)$, and $\mathrm{ECR}_{\mathrm{ub}y\_\mathrm{DO}}(i)$ are among DO tuning parameters of Figure 4.

Further details on the imposed cooperation and consistency between TOCS and DO modules formulations have been explained by the authors in [28].

Similar to TOCS, in order to include MVs and CVs status values and the additional control specifications in the DO Quadratic Programming (QP) problem, the following diagonal matrices are defined:

$$\begin{aligned} T_u &= \mathrm{diag}\left(p_u\right), \\ T_y &= \mathrm{diag}\left(p_y\right), \end{aligned} \tag{17}$$

where $\mathrm{diag}(x)$ indicates a $[n \times n]$ diagonal matrix with the element of x along the main diagonal. T_u is a $[l_u \times l_u]$ matrix and T_y is a $[m_y \times m_y]$ matrix. The initial $Q(i)$ and $S(i)$ matrices are modified as follows:

$$\begin{aligned} Q(i) &= Q(i) \circ T_y \\ S(i) &= S(i) \circ T_u. \end{aligned} \tag{18}$$

A constraint cut-off procedure similar to that described for TOCS in the previous section is then applied.

Through the solution of the QP problem, DO module computes $\Delta\widehat{u}(k+j \mid k)$ $(j = 0, \ldots, H_u - 1)$ and $\varepsilon_{\mathrm{DO}}(k)$ terms. Only the first MVs move, represented by $\Delta\widehat{u}(k \mid k)$, is considered, obtaining $u(k)$.

3.5. Stoichiometric Ratios Constraints Handling. In the previous subsections, TOCS and DO stoichiometric ratios constraints have been symbolically represented with TOCS z constraints (11)(iv) and DO z constraints (16)(iv).

In $\widehat{u}_{\mathrm{TOCS}}(k)$ and $\widehat{u}(k+j \mid k)$ $(j = 0, \ldots, H_u - 1)$ $[l_u \times 1]$ vectors, the furnace zone i fuel and air flow rates $(i = 1, \ldots, m_z)$ represent the ith and $(i + m_z)$th component $(m_z = 5)$.

The steady state formulation of the furnace zone i stoichiometric ratio $(i = 1, \ldots, 5)$ is the following:

$$\widehat{z}_{\mathrm{TOCS}_i}(k) = \frac{\widehat{u}_{\mathrm{TOCS}_{i+5}}(k)}{\widehat{u}_{\mathrm{TOCS}_i}(k)}, \tag{19}$$

where $\widehat{u}_{\mathrm{TOCS}_{i+5}}(k)$ and $\widehat{u}_{\mathrm{TOCS}_i}(k)$ represent the steady state values of furnace zone i air and fuel flow rates (nonnegative values). Denoting the steady state lower and upper constraints of furnace zone i stoichiometric ratio as $\mathrm{lb}_{z\_\mathrm{TOCS}_i}$ and $\mathrm{ub}_{z\_\mathrm{TOCS}_i}$, TOCS z constraints can be expressed by

$$\mathrm{lb}_{z\_\mathrm{TOCS}_i} \le \widehat{z}_{\mathrm{TOCS}_i}(k) \le \mathrm{ub}_{z\_\mathrm{TOCS}_i}. \tag{20}$$

Expression (20) can be recast as a set of linear inequality constraints on TOCS decision variables $\Delta\widehat{u}_{\mathrm{TOCS}}(k)$, exploiting (6). In the proposed application, stoichiometric ratios steady state constraints are assumed as *hard* constraints: they can never be violated and their feasibility has been suitably imposed. Based on rCVs final status value, when the generic ith rCV is *inactive*, all the upper and lower constraints related to the ith rCV in (20) are cut off by TOCS module.

The dynamic formulation of the generic furnace zone i stoichiometric ratio $(i = 1, \ldots, 5)$ at the jth prediction instant is the following:

$$\widehat{z}_i(k+j \mid k) = \frac{\widehat{u}_{i+5}(k+j \mid k)}{\widehat{u}_i(k+j \mid k)}, \tag{21}$$

where $\widehat{u}_{i+5}(k+j \mid k)$ and $\widehat{u}_i(k+j \mid k)$ represent the dynamic values of furnace zone i air and fuel flow rates (nonnegative values). Denoting the dynamic lower and upper constraints of furnace zone i stoichiometric ratio at the jth prediction instant as $\mathrm{lb}_{z\_\mathrm{DO}_i}(j)$ and $\mathrm{ub}_{z\_\mathrm{DO}_i}(j)$, DO z constraints can be expressed by

$$\begin{aligned} \mathrm{lb}_{z\_\mathrm{DO}_i}(j) - \mathrm{ECR}_{\mathrm{lb}z\_\mathrm{DO}_i}(j) \cdot \varepsilon_{\mathrm{DO}}(k) &\le \widehat{z}_i(k+j \mid k) \\ &\le \mathrm{ub}_{z\_\mathrm{DO}_i}(j) + \mathrm{ECR}_{\mathrm{ub}z\_\mathrm{DO}_i}(j) \cdot \varepsilon_{\mathrm{DO}}(k). \end{aligned} \tag{22}$$

Expression (22) can be recast as a set of linear inequality constraints on DO decision variables $\Delta\widehat{u}(k+j \mid k)$ $(j = 0, \ldots, H_u - 1)$ and $\varepsilon_{\mathrm{DO}}(k)$, exploiting H_u definition. In the proposed application, stoichiometric ratios dynamic constraints are assumed as *soft* constraints: their *softening* is admitted in critical situations thanks to the introduction of a suitable nonnegative slack variable for each stoichiometric ratio. These slack variables have been included in the $\varepsilon_{\mathrm{DO}}(k)$ vector. $\mathrm{ECR}_{\mathrm{lb}z\_\mathrm{DO}_i}(j)$ and $\mathrm{ECR}_{\mathrm{ub}z\_\mathrm{DO}_i}(j)$ positive vectors contain the Equal Concern for the Relaxation (ECR) coefficients. These coefficients, in cooperation with the related elements of ρ_{DO} positive definite diagonal matrix, allow a suitable constraints relaxation ranking.

Based on rCVs final status value, when the generic ith rCV is *inactive*, all the H_u upper and lower constraints related to the ith rCV in (22) are cut off by DO module.

4. Simulation Results

This section illustrates some details on tuning procedures and reports simulation examples that show the efficiency of the proposed control solutions.

4.1. Controller Tuning Summary. Through a constrained control of zones temperature, the required billets temperature at the furnace exit can be ensured; thanks to the cooperative action of TOCS and DO modules, optimal economic configurations of fuel flow rates inside the assigned process constraints can be obtained. The need of a two-layer architecture was motivated by the necessity of a steady state optimization, able to supply economic MVs targets. In addition, the developed cooperation feature between TOCS and DO modules avoids the process conduction toward dangerous operating points and/or the exhibition of inefficient transient state behaviours. A further optimization of the APC system that can deal with the various furnace conditions has been

Table 7: Considered set of MVs.

Variable name	Acronym [units]
Zone 5 fuel	Fuel_5 [Nm^3/h]
Zone 4 fuel	Fuel_4 [Nm^3/h]
Zone 5 air	Air_5 [Nm^3/h]
Zone 4 air	Air_4 [Nm^3/h]

Table 8: Considered set of CVs/rCVs.

Variable name	Acronym [units]
Zone 5 temperature	Temp_5 [°C]
Zone 4 temperature	Temp_4 [°C]
Zone 5 stoichiometric ratio	R_5 []
Zone 4 stoichiometric ratio	R_4 []

Table 9: Reduced mapping matrix.

Acronym	Fuel_5	Fuel_4	Air_5	Air_4
Temp_5	+	+	−	
Temp_4		+		−

Table 10: Reduced Decoupling Matrix D_E.

Acronym	Fuel_5	Fuel_4	Air_5	Air_4
Temp_5	1	0	0	1
Temp_4	1	1	1	0

achieved exploiting a billets reheating first-principles model [28]. Two main control modes have been formulated: the first, which has been detailed in this paper, is based on the CVs/rCVs-MVs/DVs models, while the second exploits also the billets modelization. Online parameters estimation techniques have been developed and exploited in a linear parameter varying control scheme.

In order to obtain the desired performances of the designed APC system, an accurate tuning phase of TOCS and DO modules has been conducted. Setting the APC cycle time at 1 minute, a prediction horizon of 60 minutes and a control horizon of eight moves have been selected. In this way, the considered linear time invariant model reaches a steady state condition and the controller is equipped with a suitable number of decision variables for the optimization problems [29].

In DO cost function (15), tracking objectives related to CVs have not been taken into account: $Q(i)$ matrices are all zero matrices. In TOCS and DO cost functions (10) and (15), the highest priority has been assigned to the minimization of the involved slack variables, so as to comply with CVs and rCVs constraints. For this purpose, ρ_{y_TOCS} and ρ_{DO} terms have been suitably set. In order to define a CVs/rCVs priority ranking in constraints relaxation, a joint tuning of these weights (ρ_{y_TOCS}, ρ_{DO}) and ECR coefficients has been performed. For example, smoke-exchanger temperature, total air flow rate, and stoichiometric ratios constraints are of major importance with respect to furnace zones temperature constraints. Furthermore, a joint tuning of $S(i)$ and $R(i)$ initial matrices has been performed, in order to guarantee targets reaching for all the MVs while controlling moves magnitude.

In TOCS cost function, c_u elements related to fuel flow rates have been set as positive, in order to prefer the fuels minimization direction when possible. The remaining c_u elements have been set to zero.

Finally, the initial Decoupling Matrix D_E provided by *P&S* block to *DC&DS* block has been set so as to satisfy the additional control specifications (i)–(iii) depicted in Section 2.3.

In the following Sections 4.2 and 4.3, two simulation examples are proposed showing the validity of the proposed control strategy. The proposed simulations refer to the control of zone 5 and zone 4 of the furnace. Tables 7 and 8 depict the considered process variables. Relationships between the considered MVs and CVs have been depicted in Table 9: relationships have been simply denoted with the gain sign of the related transfer function. Table 10 shows the initial Decoupling Matrix D_E provided by *P&S* block to *DC&DS* block related to the MVs and CVs at issue.

4.2. Zone 5 Control Simulation Example. The first simulation example considers to have only the furnace zone 5 under control of the proposed APC system. The other MVs, CVs, and rCVs are assumed as *inactive*, so they are not considered for control purposes; *DC&DS* block and the other modules perform all the operations related to *inactive* process variables as explained in the previous sections. In particular, all (initial) D_E rows and columns related to *inactive* CVs and MVs are zeroed by *DC&DS* block. The *inactive* MVs and all the DVs are assumed constant, so not influencing the proposed simulation.

TOCS and DO modules have to ensure an optimal usage of zone 5 fuel and air flow rates, taking into account zone 5 temperature and zone 5 stoichiometric ratio constraints. In particular, thanks to the decoupling strategy, for zone 5 temperature constraints tightening only zone 5 fuel flow rate is used, thus meeting the related specification depicted in Section 2.3.

The initial process operating point assumes that the two considered output variables (Figures 5 and 6, blue line) satisfy their constraints: in the first 30 simulation instants, the cooperative action of TOCS and DO modules ensures zone 5 fuel flow rate minimization (Figure 7, blue line), saturating zone 5 stoichiometric ratio upper bound (Figure 6, red line) and meeting zone 5 temperature constraints (Figure 5, red lines). In this first part of the simulation, no TOCS and DO modules constraints softening is required (red, cyan, and green lines in Figures 5 and 6 overlap). A profitable operating point for zone 5 fuel and air flow rates is guaranteed, saturating zone 5 air flow rate lower bound (Figures 7 and 8, blue lines). Subsequently, at time instant 31, an operator request is simulated: zone 5 temperature upper and lower constraints are increased by 50[°C] and 40[°C], respectively. Thanks to the proposed decoupling strategy, only zone 5 fuel flow rate acts for the satisfaction of the updated temperature constraints, reaching the new TOCS target (Figure 7, black line). After a brief transient, requiring a temporary softening of its new lower constraint (Figure 5, green lines), zone

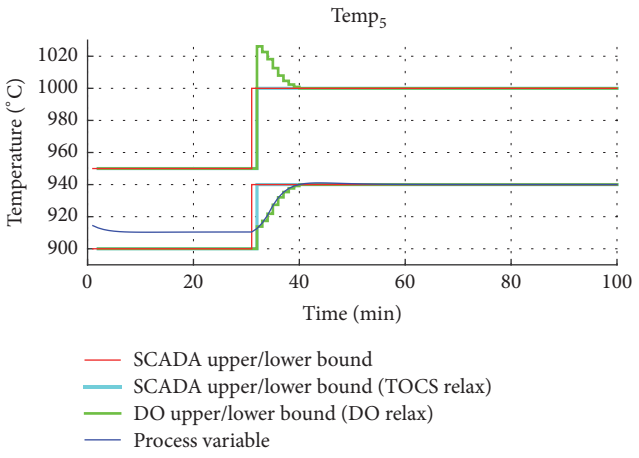

Figure 5: Zone 5 temperature trends.

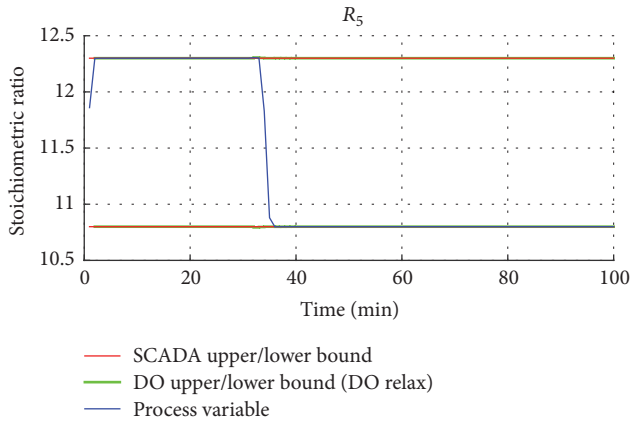

Figure 6: Zone 5 stoic. ratio trends.

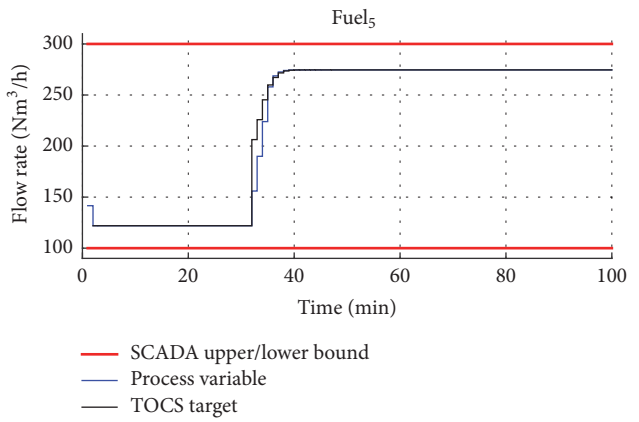

Figure 7: Zone 5 fuel flow rate trends.

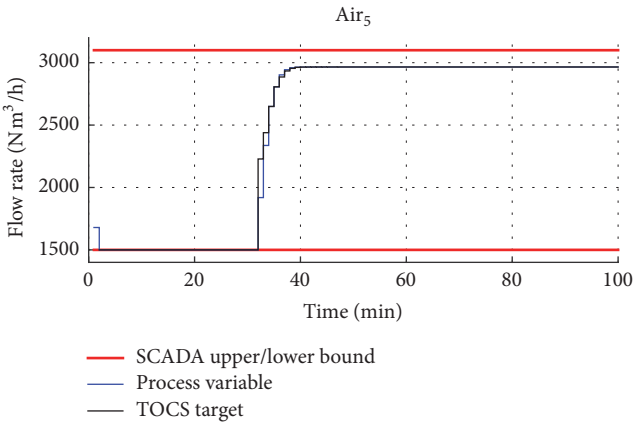

Figure 8: Zone 5 air flow rate trends.

5 temperature is restored on its new lower bound. This corrective action of zone 5 fuel flow rate could lead to the violation of zone 5 stoichiometric ratio lower bound: in order to avoid this critical condition, also zone 5 air flow rate TOCS target is changed (Figure 8, black line). In this way, zone 5 stoichiometric ratio approaches its lower bound, after a negligible DO constraints softening (Figure 6, green lines).

4.3. Zones 4 and 5 Control Simulation Example. The second simulation example considers only the furnace zones 4 and 5 under control of the proposed APC system. The other MVs, CVs, and rCVs are assumed as *inactive*, so they are not considered for control purposes; *DC&DS* block and the other modules perform all the operations related to *inactive* process variables as explained in the previous sections. In particular, all (initial) D_E rows and columns related to *inactive* CVs and MVs are zeroed by *DC&DS* block. The *inactive* MVs and all the DVs are assumed constant, so not influencing the proposed simulation.

TOCS and DO modules have to ensure an optimal usage of zones 4 and 5 fuel and air flow rates, taking into account zones 4 and 5 temperature and zones 4 and 5 stoichiometric ratios constraints. In particular, thanks to the decoupling strategy, for zone 5 temperature constraints tightening only zone 5 fuel flow rate is used, while for zone 4 temperature constraints meeting only zone 4 fuel flow rate is exploited. In this way, the related specification depicted in Section 2.3 is satisfied.

The initial process operating point assumes that the four considered output variables (Figures 9, 10, and 13, blue line) satisfy their constraints (zone 4 temperature has not been depicted for brevity): in the first 20 simulation instants, the cooperative action of TOCS and DO modules ensures zone 5 and zone 4 fuel flow rate minimization (Figures 12 and 14, blue line), saturating zone 5 stoichiometric ratio upper bound (Figure 10, red line) and meeting zone 4 stoichiometric ratio constraints (Figure 13, red lines). Furthermore, in this first part of simulation, zones 4-5 temperature meets the imposed constraints (Figure 9, red lines) and no TOCS and DO modules constraints softening is required (red, cyan, and green lines in Figures 9, 10, and 13 overlap). A profitable operating point for zones 4-5 fuel and air flow rates is guaranteed, saturating zone 5 air flow rate lower bound (Figures 11, 12, and 14, blue lines; zone 4 air flow rate has not been depicted for brevity: it remains constant at its initial value during the simulation). Subsequently, at time instant 21, an operator request is simulated: zone 5 temperature lower constraint

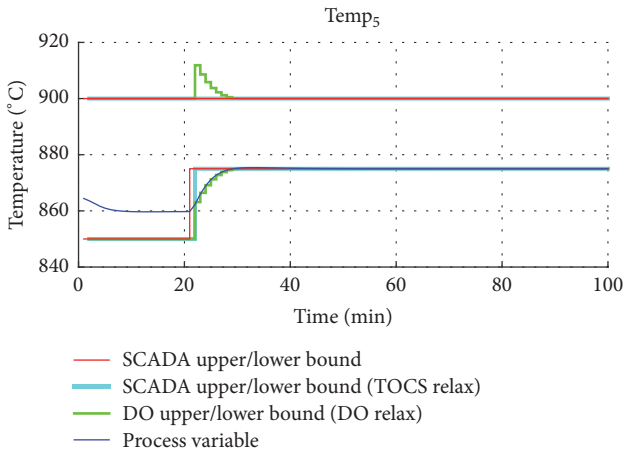

Figure 9: Zone 5 temperature trends.

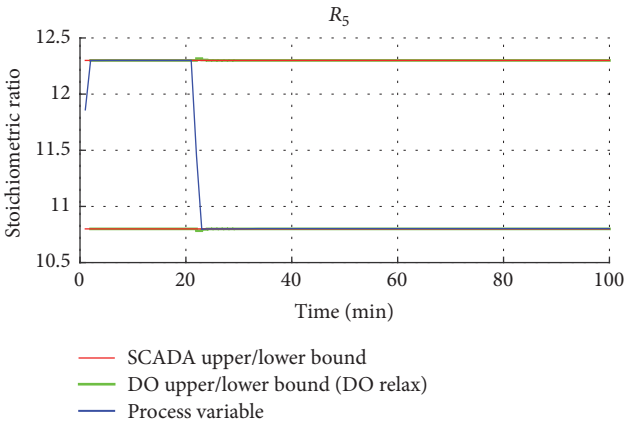

Figure 10: Zone 5 stoic. ratio trends.

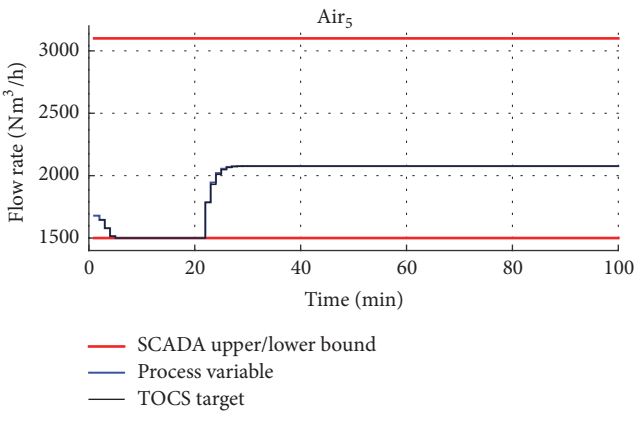

Figure 11: Zone 5 air flow rate trends.

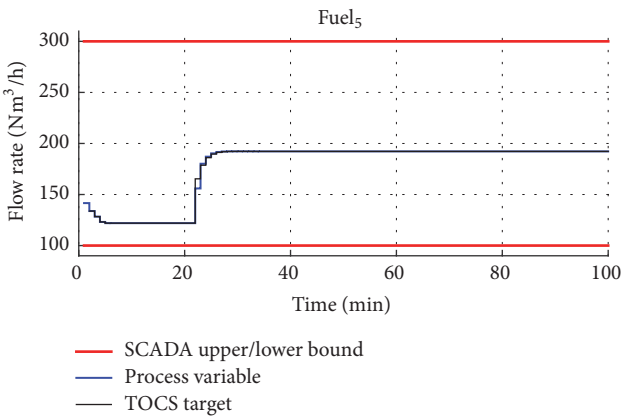

Figure 12: Zone 5 fuel flow rate trends.

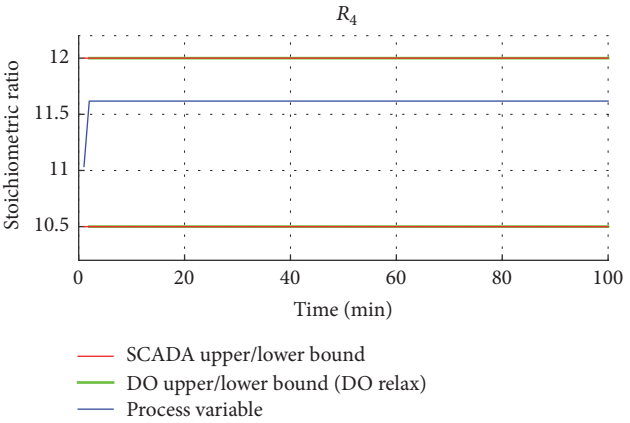

Figure 13: Zone 4 stoic. ratio trends.

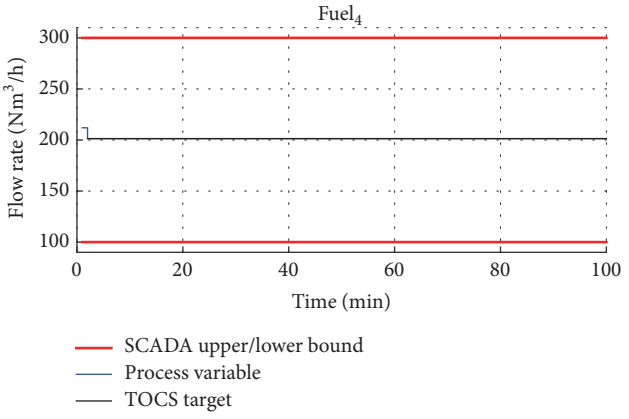

Figure 14: Zone 4 fuel flow rate trends.

is increased by 25[°C]. Thanks to the proposed decoupling strategy, only zone 5 fuel flow rate acts for the satisfaction of the updated temperature constraints, reaching the new TOCS target (Figure 12, black line). After a brief transient, requiring a temporary softening of its new lower constraint (Figure 9, green lines), zone 5 temperature is restored on its new lower bound. This corrective action of zone 5 fuel flow rate could lead to the violation of zone 5 stoichiometric ratio lower bound: in order to avoid this critical condition, also zone 5 air flow rate TOCS target is changed (Figure 11, black line). In this way, zone 5 stoichiometric ratio approaches its lower bound, after a negligible DO constraints softening (Figure 10, green lines). Note that the proposed constraint change does not modify zone 4 variables configuration.

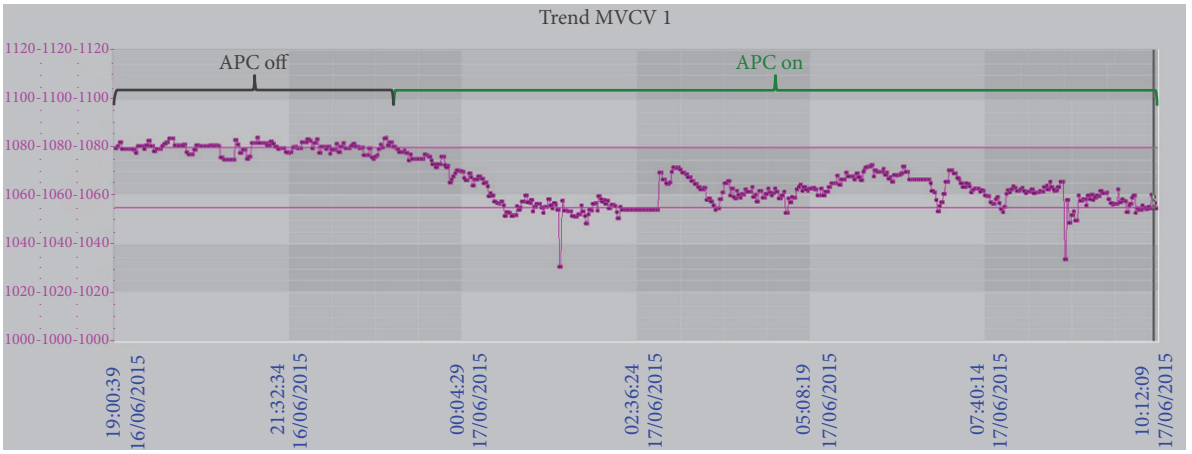

Figure 15: Billets final temperature trends and related constraints.

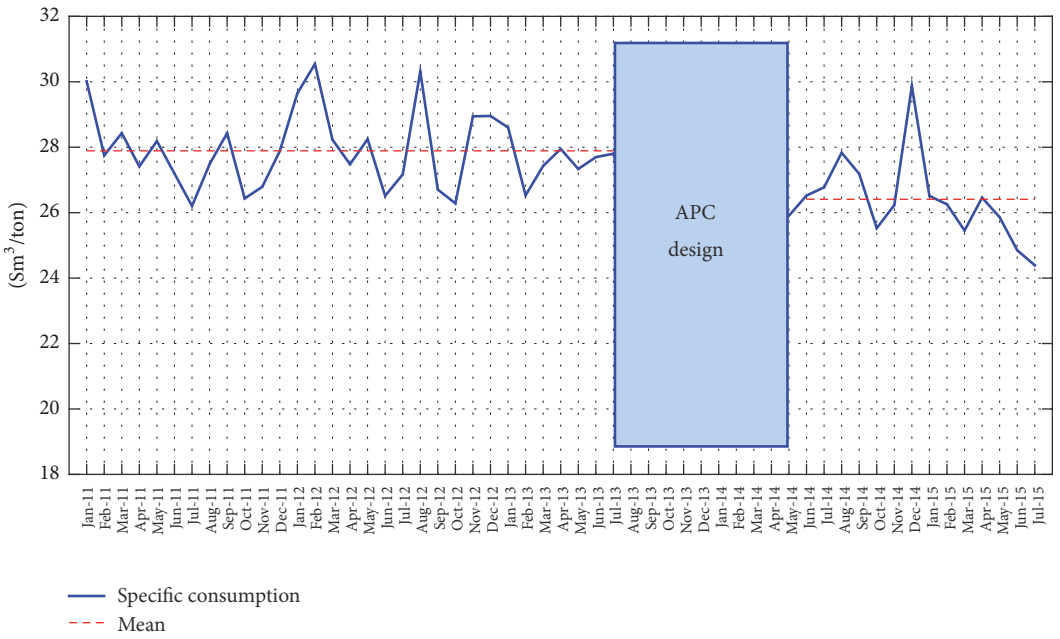

Figure 16: Fuel specific consumption trends and related expected values without and with the designed APC system.

5. Field Results

The project for the realization of the proposed APC system began in August 2013 and ended in May 2014, through a profitable cooperation between Università Politecnica delle Marche and i.Process Srl. Together with an additional billets first principle model, the whole work has been introduced in proprietary software and it has been awarded with an Italian patent [15].

The introduction of the APC system on the real plant dates back to early June 2014, replacing operators' manual conduction of local PID controllers.

Figure 15 shows an example of the plant performances with the designed control system comparing them with the previous control system ones. The billets final temperature measured by the optical pyrometer is depicted for a total period of 15 hours. Similar furnace boundary conditions (e.g., billets input temperature and furnace production rate) are considered. The first 4 hours refer to the previous control system conduction (APC OFF): with this control solution, the billets temperature constraints at the exit of the furnace (straight lines, 1055[°C]–1080[°C]) are met, but energy saving and environmental impact decreasing aspects are neglected. In fact, final billets temperature often results in being very close to the imposed upper bound. In the following 11 hours, the controller is switched to the designed one (APC ON): as it can be noted, the billets final temperature approaches its lower bound thus leading to energy efficiency achievement.

In Figure 16, the fuel specific consumption ([Sm^3/ton]) before and after the introduction of the designed control system is depicted. The fuel specific consumption is computed considering natural gas usage and furnace production rate.

A period of four and a half years is taken into account. The period from January 2011 to July 2013 (at the left side of Figure 16) refers to the previous control system, while the one from June 2014 to May 2015 (at the right side of Figure 16) is related to the proposed APC system. As shown in Figure 16, about 5% reduction is observed after the activation of the designed control system. Up to June 2016, the reduction has become greater than 6%. Furthermore, after two years from the first startup, a service factor greater than 95% has been registered.

6. Conclusions

In this work, the control and optimization of a walking beam billets reheating furnace located in an Italian steel plant have been addressed.

An Advanced Process Control architecture, based on a two-layer linear Model Predictive Control strategy, has been developed. Suitable modifications on the mathematical formulations of the two layers have been proposed, in order to comply with the required control specifications, and two control solutions have been detailed. An extended decoupling strategy has been formulated assuring, in all process conditions and independently on tuning parameters, a unified approach to the problem of the selection of the input variables to exploit for the control of each single output variable. For this purpose, an ad hoc module has been introduced. In addition, a tailored stoichiometric ratios constraints formulation has been introduced into the two Model Predictive Control layers.

Simulation results demonstrated the validity and the reliability of the proposed control solutions.

Field results have shown the advantages of the introduction of the designed Advanced Process Control system on the real plant, substituting the previous operators' manual conduction of local PID controllers: energy saving and environmental impact decreasing aspects have been optimized, thus leading to a major energy efficiency.

The considered strategy has been introduced in a proprietary tool, obtaining an Italian patent.

Competing Interests

The authors declare that there is no conflict of interests regarding the publication of this paper.

References

[1] http://www.honeywellprocess.com.

[2] M. Bauer and I. K. Craig, "Economic assessment of advanced process control—a survey and framework," *Journal of Process Control*, vol. 18, no. 1, pp. 2–18, 2008.

[3] P. L. Latour, J. H. Sharpe, and M. C. Delaney, "Estimating benefits from advanced control," *ISA Transactions*, vol. 25, no. 4, pp. 13–21, 1986.

[4] C. R. Cutler and B. L. Ramaker, "Dynamic matrix control—a computer control algorithm," in *Proceedings of the Dynamic matrix controla computer control algorithm*, 1980.

[5] S. J. Qin and T. A. Badgwell, "A survey of industrial model predictive control technology," *Control Engineering Practice*, vol. 11, no. 7, pp. 733–764, 2003.

[6] Y. G. Xi, D. W. Li, and S. Lin, "Model predictive control—current status and challenges," *Acta Automatica Sinica*, vol. 39, no. 3, pp. 222–236, 2013.

[7] M. L. Darby and M. Nikolaou, "MPC: current practice and challenges," *Control Engineering Practice*, vol. 20, no. 4, pp. 328–342, 2012.

[8] B. Lede, "A control system for fuel optimization of reheating furnaces," *Scandinavian Journal of Metallurgy*, vol. 15, no. 1, pp. 16–24, 1986.

[9] Z. Wang, T. Chai, S. Guan, and C. Shao, "Hybrid optimization setpoint strategy for slab reheating furnace temperature," in *Proceedings of the American Control Conference (ACC '99)*, pp. 4082–4086, San Diego, Calif, USA, June 1999.

[10] H. S. Ko, J.-S. Kim, T.-W. Yoon, M. Lim, D. R. Yang, and I. S. Jun, "Modeling and predictive control of a reheating furnace," in *Proceedings of the American Control Conference*, pp. 2725–2729, June 2000.

[11] L. Balbis, J. Balderud, and M. J. Grimble, "Nonlinear predictive control of steel slab reheating furnace," in *Proceedings of the American Control Conference (ACC '08)*, pp. 1679–1684, Seattle, Wash, USA, June 2008.

[12] A. Steinboeck, D. Wild, and A. Kugi, "Feedback tracking control of continuous reheating furnaces," in *Proceedings of the 18th IFAC World Congress*, pp. 11744–11749, Milano, Italy, September 2011.

[13] A. Steinboeck, D. Wild, and A. Kugi, "Nonlinear model predictive control of a continuous slab reheating furnace," *Control Engineering Practice*, vol. 21, no. 4, pp. 495–508, 2013.

[14] Y. Zheng, N. Li, and S. Li, "Hot-rolled strip laminar cooling process plant-wide temperature monitoring and control," *Control Engineering Practice*, vol. 21, no. 1, pp. 23–30, 2013.

[15] L. Barboni, G. Astolfi, C. Pepe, and F. Cocchioni, "Metodo Per Il Controllo Di Forni Di Riscaldo," Italian Patent n. 0001424136 awarded by Ufficio Italiano Brevetti e Marchi (UIBM), 2014 http://www.uibm.gov.it/uibm/dati/Avanzata.aspx?load=info_list_uno&id=2253683&table=Invention&.

[16] S. M. Zanoli, C. Pepe, and L. Barboni, "Application of advanced process control techniques to a pusher type reheating furnace," *Journal of Physics: Conference Series*, vol. 659, no. 1, 2015.

[17] W. Trinks, M. H. Mawhinney, R. A. Shannon, R. J. Reed, and J. R. Garvey, *Industrial Furnaces*, John Wiley & Sons, New York, NY, USA, 2004.

[18] A. von Starck, A. Muhlbauer, and C. Kramer, *Handbook of Thermoprocessing Technologies*, Vulkan, Essen, Germany, 2005.

[19] A. Martensson, "Energy efficiency improvement by measurement and control: a case study of reheating furnaces in the steel industry," in *Proceedings of the 14th National Industrial Energy technology Conference*, pp. 236–243, 1992.

[20] F. G. Shinskey, *Energy Conservation Through Control*, Academic Press, New York, NY, USA, 1978.

[21] L. Ljung, *System Identification: Theory for the User*, Prentice-Hall, Englewood Cliffs, NJ, USA, 1987.

[22] *Multivariable system identification for process control*, Elsevier, 2001.

[23] T. Liu, Q.-G. Wang, and H.-P. Huang, "A tutorial review on process identification from step or relay feedback test," *Journal of Process Control*, vol. 23, no. 10, pp. 1597–1623, 2013.

[24] C. Pepe and S. M. Zanoli, "A two-layer model predictive control system with adaptation to variables status values," in *Proceedings of the 17th IEEE International Carpathian Control Conference (ICCC '16)*, pp. 573–578, High Tatras, Slovakia, May 2016.

[25] J. Maciejowski, *Predictive Control with Constraints*, Prentice-Hall, Harlow, UK, 2002.

[26] E. F. Camacho and C. A. Bordons, *Model Predictive Control*, Springer, London, UK, 2007.

[27] J. B. Rawlings and D. Q. Mayne, *Model Predictive Control: Theory and Design*, Nob Hill, Madison, Wisc, USA, 2013.

[28] S. M. Zanoli and C. Pepe, "The importance of cooperation and consistency in two-layer Model Predictive Control," in *Proceedings of the 17th IEEE International Carpathian Control Conference (ICCC '16)*, pp. 825–830, High Tatras, Slovakia, May 2016.

[29] J. L. Garriga and M. Soroush, "Model predictive control tuning methods: a review," *Industrial & Engineering Chemistry Research*, vol. 49, no. 8, pp. 3505–3515, 2010.